Catalysis Today 258 (2015) 35–40

Contents lists available at ScienceDirect

Catalysis Today

journal homepage: www.elsevier.com/locate/cattod

The role of Ag—O—Al entities in adsorption of —NCO species and reduction of NO_x

Hua Deng, Yunbo Yu, Hong He*

State Key Joint Laboratory of Environment Simulation and Pollution Control, Research Center for Eco-Environmental Sciences, Chinese Academy of Sciences, Beijing 100085, China

ARTICLE INFO

Article history:
Received 10 December 2014
Received in revised form 3 February 2015
Accepted 5 March 2015
Available online 14 April 2015

Keywords:
Ag/Al_2O_3
NO_x
SCR
DFT
NMR
EXAFS

ABSTRACT

In order to investigate the selective catalytic reduction of NO_x by hydrocarbons, Ag/Al_2O_3 models were constructed by means of density functional theory (DFT) and experimental results. The geometrical structures and vibrational frequencies obtained at B3LYP levels of DFT were compared with the corresponding experimental results. EXAFS results suggest silver ion species were predominant on the Al_2O_3 surface. Two forms of interaction between Ag and the Al_2O_3 support can be deduced, namely Ag—O—Al_{octa} (octahedral, AlO_6) and Ag—O—Al_{tetra} (tetrahedral, AlO_4). The Ag—O—Al_{octa} interaction is energetically favorable, which can be corroborated by both NMR results and DFT calculation. However, vital —NCO intermediate species prefer to adsorb on the Ag—O—Al_{tetra} entity. In the reduction of NO_2, —NCO species close to Ag—O—Al_{tetra} are more favorable than those on Ag—O—Al_{octa}, both energetically and kinetically. Thus Ag—O—Al_{tetra} rather than Ag—O—Al_{octa} should be considered as the active site during the HC-SCR process. The CNO— species, as an isomer of —NCO, was also examined by theoretical methods, and it was found to be more kinetically favorable to reduce NO_x over the site of the Ag—O—Al_{tetra} entity than —NCO species.

1. Introduction

NO_x removal from lean-burn exhaust remains a major challenge in environmental catalysis. Selective catalytic reduction of NO_x by hydrocarbons (HC-SCR) is a potential method to remove NO_x from lean-burn exhausts [1–5]. The alumina supported silver catalyst (Ag/Al_2O_3) is deemed one of the most effective materials for HC-SCR of NO_x in excess oxygen [6–10]. In particular, ethanol is extremely effective for the SCR of NO_x over Ag/Al_2O_3 [11]. As a result, many efforts have been made to draw a relationship between the structural features of Ag/Al_2O_3 catalysts and their catalytic activity in the SCR of NO_x.

Serving as a support for silver, Al_2O_3 is better than other oxide supports like TiO_2, SiO_2, etc. [12,13]. For HC-SCR over Ag/Al_2O_3, it has been accepted that silver (Ag) and support Al must interact strongly with each other to guarantee high activity in NO_x reduction. For instance, kinetic measurements performed by She and Flytzani-Stephanopoulos [14] confirmed that silver species, particularly Ag^+ cations strongly bound with the alumina support and possibly present as [Ag—O—Al] entities, are the active sites for SCR of NO_x with methane. Furthermore, using in situ DRIFTS and DFT calculation, Yan et al. [15] proposed that reactive enolic species prefer to adsorb on Ag sites or the interface between silver and the support. More recently, based on theoretical simulation of the local structure of silver species and its interface with the support [16], we found that the orbital mixing among Ag, O and Al in Ag/Al_2O_3 is vital for the excellent catalytic performance of Ag/Al_2O_3. The results mentioned above suggest that the interaction of silver species with alumina is a key issue for revealing the intrinsic properties that enable HC-SCR over Ag/Al_2O_3 with high efficiency. Nevertheless, the alumina support generally has different Al coordination environments, such as Al octahedral (AlO_6) and/or tetrahedral (AlO_4) coordination sites, on which the silver species location and the corresponding activity remain an open question.

Isocyanate (—NCO) is widely accepted as a vital intermediate when carbon monoxide and a variety of hydrocarbons are used as reducing agents. The assignment of —NCO can be traced back a long time. For instance, London and Bell [17] carried out a simultaneous infrared and kinetic study of the reduction of NO_x by CO in 1973. A band at 2200 cm^{-1} was attributed to an interaction between NO and CO, moreover, the observed band at 2200 cm^{-1} is very close to pseudo-antisymmetric stretching vibrations of —NCO in tetraethylammonium tetraisocyantatocuprate (2198 cm^{-1}). Based upon this strong indication, the assignment of the band around 2200 cm^{-1}

* Corresponding author. Tel.: +86 10 6284 9123.
E-mail address: honghe@rcees.ac.cn (H. He).

http://dx.doi.org/10.1016/j.cattod.2015.03.023
0920-5861/

to M^+—NCO species was confirmed. Using hydrocarbons such as propylene as reducing agents, a surface isocyanate intermediate (band observed in the range 2180–2270 cm^{-1}) was also found by Ukisu et al. [18] in 1991. Henceforth, the —NCO species was identified as a surface intermediate during the reduction of NO_x.

The activity of —NCO species was carefully examined by many groups [19,20]. Sumiya et al. [19] studied the reactivity of isocyanate species over Ag/Al_2O_3. Two types of —NCO species (on Ag and Al_2O_3) were formed, which are thermally stable in vacuum at 673 K. However, —NCO species are more reactive in a mixture of $NO + O_2$ than in NO or O_2 alone, being eventually converted into N_2, CO_2 and CO. Using short time-on-stream in situ spectroscopic transient isotope experimental techniques (STOS-SSITKA), Burch et al. [21,22] differentiated the types of isocyanate species. It was found that the slowly reacting spectator isocyanate species is probably adsorbed on the oxide support, and the reactive one possibly on or close to the active silver phase.

Isocyanate species may arise from the thermal decomposition of a precursor complex, $NO_xC_yH_z$, during reduction of NO_x by hydrocarbons. Concerning the formation of —NCO species, an approximate mechanism is proposed whereby $NO + O_2 + C_xH_y \rightarrow NO_x$ (such as nitrates) + $C_xH_yO_z$ (such as acetate and enolic species) → R—NO_2 + R—ONO → —NCO + —CN. In particular, nitrates and enolic species could be key precursors in the formation of —NCO during NO_x reduction by oxygenated hydrocarbons [11]. Tamm et al. [23] investigated the —NCO and —CN intermediates in the reaction path in HC-SCR. Two parallel independent reaction pathways for —NCO and —CN species to reduce NO_x were proposed. Other works [24,25] came to different conclusions about the two intermediates mentioned above. For example, Bion et al. [24] investigated the reduction of NO_x by ethanol over Ag/Al_2O_3 by in situ FTIR spectroscopy. They proposed that the formation of silver cyanide (—CN) is the precursor step in the formation of —NCO species, where the —CN species transfer from Ag^+ to Al^{3+} tetra to form Al^{3+} tetra NCO. Using a real-time infrared method, King et al. [25] proved the cyanide flip on the silver–alumina catalyst to form —NCO species. With a lifetime of 2 ms, the flip of a cyanide group from a silver nanoparticle to alumina confirms the central role of the interface between metal particles and the oxide support. Close to —CN species, fulminate species (CNO—) are isomers of —NCO species. However, the roles of CNO— in isomerization to NCO— and in reduction of NO_x have been little reported.

In this study, the predominant silver ion species anchored on Al_{octa} and/or Al_{tetra} sites are constructed by the DFT method. The Al_{octa} site is energetically favorable to anchor silver and form the Ag—O—Al_{oct} entity. However, the Ag—O—Al_{tetra} entity is beneficial for adsorbing —NCO species. Moreover, —NCO species close to an Ag—O—Al_{tetra} entity are more active than those on Ag—O—Al_{octa}. Similar activity is found between isomers of —NCO and CNO— species in the reduction of NO_x.

2. Materials and methods

2.1. Experimental section

$Ag/\gamma\text{-}Al_2O_3$ catalysts with appropriate silver loadings (1 wt% loading) were prepared by an impregnation method (surface area = 148.5 m^2/g) [26]. An appropriate amount of $\gamma\text{-}Al_2O_3$ (Sigma–Aldrich, 199974-1KG, activated, neutral, Brockmann) was immersed into an aqueous solution of silver nitrate (Sinopharm Chemical Reagent Co., Ltd., 1008461). After stirring for 1 h, the excess water was removed by a rotary evaporator under vacuum at 333 K. Then the sample was calcined in a furnace at 873 K for 3 h. For convenience of comparison, the same procedures were followed for pure $\gamma\text{-}Al_2O_3$ (surface area = 167.3 m^2/g).

2.2. Catalytic measurements

A gaseous mixture of NO (800 ppm), C_2H_5OH (1565 ppm), water vapor (10%), and O_2 (10%) in N_2 balance at a mass flow of 1 L min^{-1} was fed as described in our earlier studies [15,16]. The catalytic activity was measured in a fixed-bed reactor, where Ag/Al_2O_3 catalyst with weight of 0.3 g was packed in the bed (GHSV = 100,000 h^{-1}). The concentrations of NO, NO_2, N_2O, NH_3, and CO were analyzed online simultaneously by an FTIR spectrometer (Nicolet Nexus is 10). In all the experiments, the concentration of N_2O was negligible, thus, NO_x conversion can be calculated using the following equation:

$$NO_x \text{ conversion } (\%) = \frac{[NO]_{in} + [NO_2]_{in} - [NO]_{out} - [NO_2]_{out}}{[NO]_{in} + [NO_2]_{in}} \times 100\%.$$

The N_2 selectivity was defined as follows:

$$N_2 \text{ selectivity } (\%) = \frac{[NO]_{in} + [NO_2]_{in} - [NO]_{out} - [NO_2]_{out} - [NH_3]_{out}}{[NO]_{in} + [NO_2]_{in}} \times 100\%.$$

2.3. Catalysts characterization

All ^{27}Al MAS NMR experiments were performed at room temperature on a Bruker 400 MHz WB solid-state NMR spectrometer, operating at a magnetic field of 9.4 T. The corresponding ^{27}Al Larmor frequency was 104.29 MHz. All of the spectra were acquired at a sample spinning rate of 10 kHz. A single pulse sequence with a pulse width of about 15° was used. Each spectrum was acquired using a total of 2000 scans with a recycle delay time of 0.5 s and an acquisition time of 0.018 s. All spectra were externally referenced (i.e., the 0 ppm position) to a 1 M $Al(NO)_3$ aqueous solution. The raw spectrum data were normalized by the weights, where constant or known weights of samples were recorded.

The EXAFS of Ag–K edges were measured in transmission mode at room temperature on the NW10A beam line, Photon Factory, Advanced Ring for pulse X-rays (PF-AR), Institute of Materials Structure Science, High Energy Accelerator Research Organization (IMSS-KEK), Japan. Ag foil and $AgNO_3$ were used as references. The storage ring was operated at 6.5 GeV with 50 mA as an average storage current. The synchrotron radiation beam line was monochromatized with a Si (3 1 1) double crystal monochromator, and mirrors were used to eliminate higher harmonics. The incident and transmitted beam intensities were monitored using ionization chambers filled with air at room temperature. After the calcination process, all samples were finely ground first. Then a self-supported wafer form of the sample (100–150 mg) with a ca. 13 mm diameter was made for X-ray absorption tests. Every sample was measured for 15–20 min.

The XAFS data were analyzed by the REX2000 program (Rigaku Co.). EXAFS oscillation $\chi(k)$ was extracted using spline smoothing and weighted by k^3 to compensate for the diminishing amplitude in the high k range. The filtered k^3 weighted $\chi(k)$ was transformed to R space in the k range of 2–9 $Å^{-1}$ with a Hanning function window. The structural parameters of the series of catalysts were obtained through curve fitting procedures using FEFF8.4 code [27].

2.4. Computational section

Minimum energy structures were calculated with the Gaussian09 program. The optimized structures and corresponding properties of the models were determined through the application of the density functional theory (DFT), using the B3LYP gradient

corrected function. The LANL2DZ effective core potential basis set was used for all of the calculations. Stability calculations confirmed the ground-state configuration of all the wave functions. The calculated vibration frequencies and infrared intensity of the vibrational normal modes were determined using GaussView 5.0.8. Adsorption energies of AgO_2 clusters on the Al_2O_3 surface are calculated using the following equations:

$$\Delta E = E(Ag/Al_2O_3) - E(AgO_2) - E(Al_2O_3).$$

3. Results and discussion

3.1. The model of Ag/Al_2O_3

Alumina is one of the most commonly used materials as a catalyst or catalyst support. Due to its importance in a wide range of catalytic reactions, properties of alumina have been the subject of many investigations. The coordination of Al atoms on alumina surfaces is of particular importance because valence-unsaturated surface Al atoms are a source of surface Lewis acidity, which is important to catalysis. Fig. 1(A) shows the ^{27}Al MAS NMR spectra of γ-Al_2O_3. The experimental NMR spectrum exhibited two main stable peaks at 7.5 and 65 ppm, which were assigned to AlO_6 (Al octahedral) and AlO_4 (Al tetrahedral) units in γ-Al_2O_3 respectively [28–31]. As shown in Fig. 1(A), the structure of γ-Al_2O_3 consists of octahedral and tetrahedral Al in proportions about 3:1, which is consistent with other works [28,29]. Based on this important result, we constructed the surface model of the support Al_2O_3. Model Al_4O_{15} contains one AlO_4 and three AlO_6 units and the dangling bonds were covered by H atoms. First, a structural optimization calculation was performed (as shown in Fig. S1). The Al—O bonds ranged from 1.812 to 2.050 Å, which is in good agreement with Digne's bulk structure of γ-Al_2O_3 (from 1.82 to 1.94 Å) [32,33].

As for the Ag/Al_2O_3 catalyst, the silver species hold the key to the HC-SCR process. It is widely accepted that different kinds of Ag species, such as isolated Ag^+ cations, oxidized silver clusters ($Ag_n^{\delta+}$), and metallic silver clusters (Ag_n^0), are present on Ag/Al_2O_3 catalysts as prepared and during HC-SCR [14,26,34–38]. Among them, oxidized silver (Ag^+ and/or $Ag_n^{\delta+}$) is believed to be the active species for NO_x reaction by hydrocarbons [14,26,34,35,37,38]. At silver loading below 2 wt%, the Ag—O shell was predominant [16]. Fig. 1(B) exhibits the Fourier transforms of k^3-weighted EXAFS oscillations at the Ag K-edge for the 1 wt% Ag/Al_2O_3 catalyst, which has shown the best NO_x reduction efficiency in this study (as shown in Fig. S2). A bond distance of Ag—O in the range of 1.75–2.5 Å was observed, with a coordination number of about ca. 3. This suggests that each silver ion species is surrounded by about 3 oxygen atoms.

The metal–support interaction is often seen as critical to sustaining high catalytic activity under demanding catalyst operation conditions. In order to understand the interaction between silver and Al_2O_3, we compared the pure support Al_2O_3 and Ag/Al_2O_3 calcined at 600 °C by ^{27}Al MAS NMR characterization. It can be clearly seen in Fig. 1(C) that the Al_{penta} site [28–31] (AlO_5 centered at 35 ppm) disappeared after silver loading and Al_{octa} increased at the same time. Thus we can conclude that the Al_{penta} site is the anchoring site for silver ions to form the Ag—O—Al_{octa} entity. Other studies also suggested that the Al_{penta} site is the anchoring site for the noble metal Pt [31]. The possible mechanism is that Ag^+ ion exchanges with the proton from hydroxyl groups bonded to the Al_{octa} site, the occurrence of which prohibits the formation of the Al_{penta} structure via dehydration of hydroxyl. On the other hand, the peak of Al_{tetra} was almost unchanged after silver loading, as shown in Fig. 1(C). However, we cannot exclude the possibility that Ag^+ ion can be stabilized on the Al_{tetra} site via exchange with the proton from a hydroxyl group bonded to the Al site. In summary, the role of Al_{tetra} in anchoring silver species has been poorly understood up to now. In order to learn the stable Al site in anchoring silver species, the first-principles method was used to constructed Ag—O—Al_{octa} and Ag—O—Al_{tetra} entities as shown in Fig. 2.

The adsorption energies for Ag—O—Al_{octa} and Ag—O—Al_{tetra} entities were −3.917 and −3.318 eV respectively. The negative ΔE values indicate that the adsorbed state is energetically favorable. Thus Ag—O—Al_{octa} is more stable than Ag—O—Al_{tetra} and should be the typical Ag—O—Al entity, which is consistent with previous characterization and former studies [31]. After silver was anchored on the Al_2O_3 surface, the Mulliken charge of Ag in Ag—O—Al_{octa} and Ag—O—Al_{tetra} entities were 0.615 and 0.621*e*, respectively. This suggests that both silver species are in the +1 oxidized states. In order to understand the chemical activity of both Ag—O—Al entities, the adsorbed vital intermediate —NCO species were calculated on Ag/Al_2O_3 in the following section.

3.2. NCO and CNO— adsorbed species on Ag/Al_2O_3

It is well known that at the heart of HC-SCR of NO_x over the Ag/Al_2O_3 catalyst is the surface mechanism. With this in mind, the vital intermediate —NCO species adsorbed on two kinds of Ag—O—Al entities were calculated to identify the active site of the Ag/Al_2O_3 catalyst. The optimized structures are displayed in Fig. 3 and the energy, structure parameters, and vibrational frequencies are listed in Table 1. According to the crystal structure of silver cyanate [39], the silver is linearly coordinated with an N atom at 2.115 Å, and bond distances between N═C and C═O are 1.195 and 1.180 Å, respectively. Our calculated model structure parameters as shown in Table 1 are very close to the results. Furthermore, it can be clearly seen that our simulated vibrational models are consistent with our experimental results (Fig. S3) and also in agreement with previous research [17–25]. The stretching modes of —NCO species on Ag—O—Al_{octa} and Ag—O—Al_{tetra} were at 2248 and 2221 cm^{-1} respectively in this study. The distances between Ag and N atoms of —NCO species are 2.083 and 2.024 Å on Ag—O—Al_{octa} and Ag—O—Al_{tetra} entities respectively as shown in Fig. 3. It is clear that the observed stretching mode of —NCO species is an asymmetric stretching vibration among the atoms C, N, and O. Since the bond length of N═C is the same in both cases as shown in Fig. 3, the C═O bond distance is critical in determining the vibration frequency of —NCO. Nevertheless, the role of silver species in shifting the vibration frequency of —NCO species is unclear. Other works also reported that —NCO species usually have a vibrational stretching mode at 2220–2260 cm^{-1} [17–25,40–42]. According to Burch et al. [21,22], a lower value of —NCO IR wavenumber indicates —NCO species adsorbed closer to an active silver site, acting as a reactive species for reducing NO_x. Comparing the two possible active silver sites, the Ag—O—Al_{tetra} entity is more favorable for the adsorption of —NCO species due to its lower total energy as shown in Table 1. However, it is still open to question whether the Ag—O—Al_{tetra} entity is more active for NO_x reduction than the Ag—O—Al_{octa} entity.

Silver fulminate and silver cyanate or isocyanates provided the first example of isomerism by Liebig and Gay-Lussac [39]. Adsorbed fulminate species (CNO—) on the silver of Ag/Al_2O_3 is assumed to form during the HC-SCR process alongside the formation of —NCO species. However, few studies have paid attention to this subject. Given the unstable properties of CNO— species, it is hard to capture their nature by direction experimental methods. Thus the theoretical method was used to learn the structure and chemistry of CNO— species on active silver sites.

The optimized adsorbed CNO— species on Ag—O—Al_{octa} and Ag—O—Al_{tetra} entities are displayed in Fig. 4 and the energy and structure parameters are also summarized in Table 1. According to the crystal structure of silver fulminate [43], the silver is linearly coordinated with an O atom at 2.447 Å, and bond distances

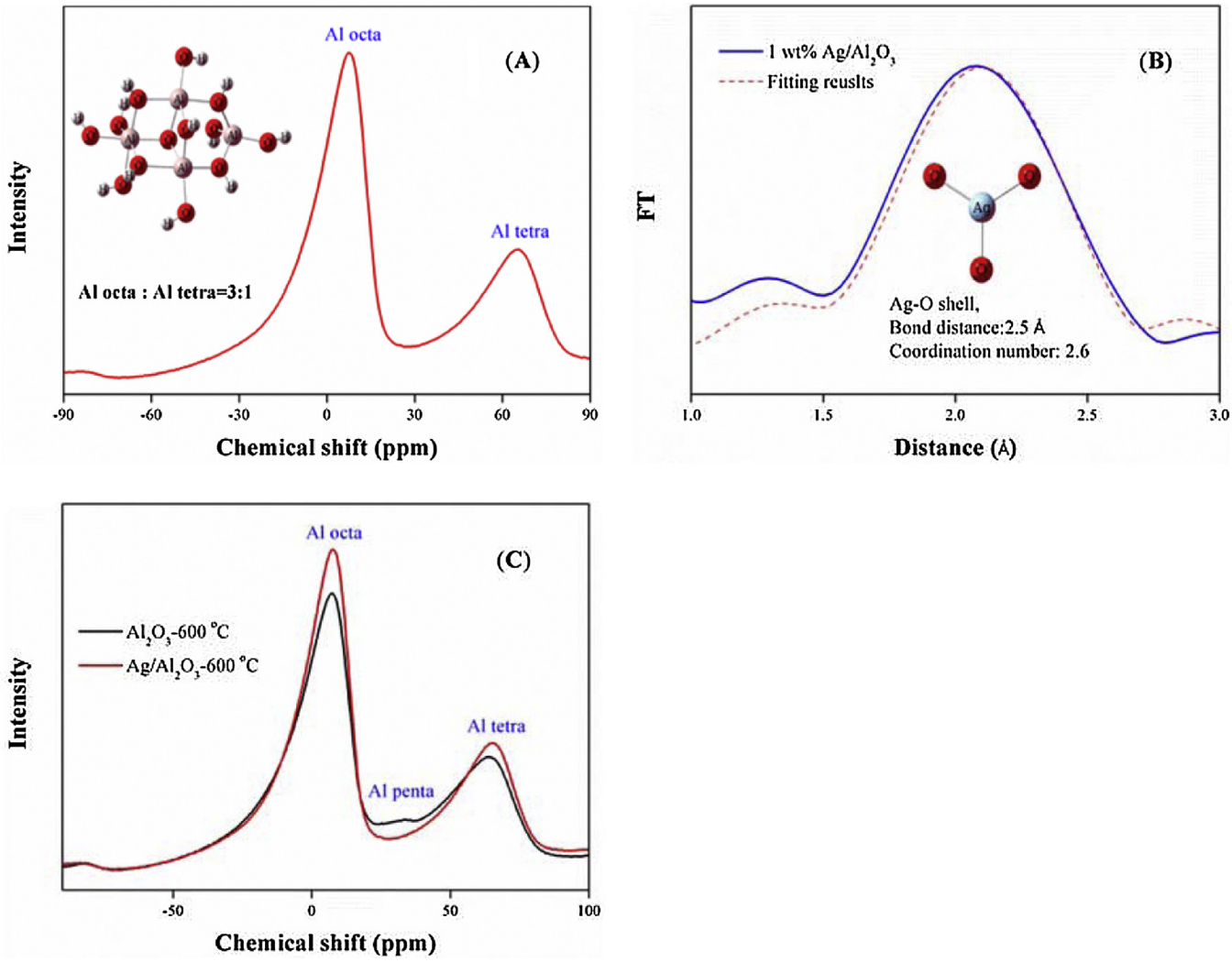

Fig. 1. (A) Solid-state ^{27}Al MAS NMR spectra of bare support Al_2O_3. (B) Comparison of the experimental and fitted pseudo-radial distribution functions from 1 wt% Ag/Al_2O_3 catalyst. (C) Solid-state ^{27}Al MAS NMR spectra of Ag/Al_2O_3 catalysts and corresponding supports calcined at 600 °C.

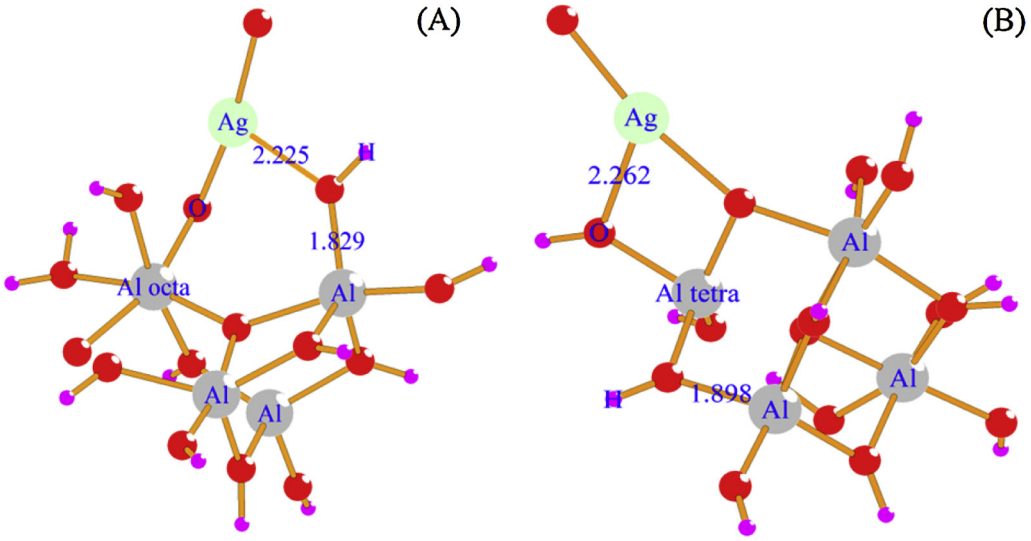

Fig. 2. Calculated models for Ag/Al_2O_3 catalyst, (A) Ag—O—Al_{octa}, (B) Ag—O—Al_{tetra}.

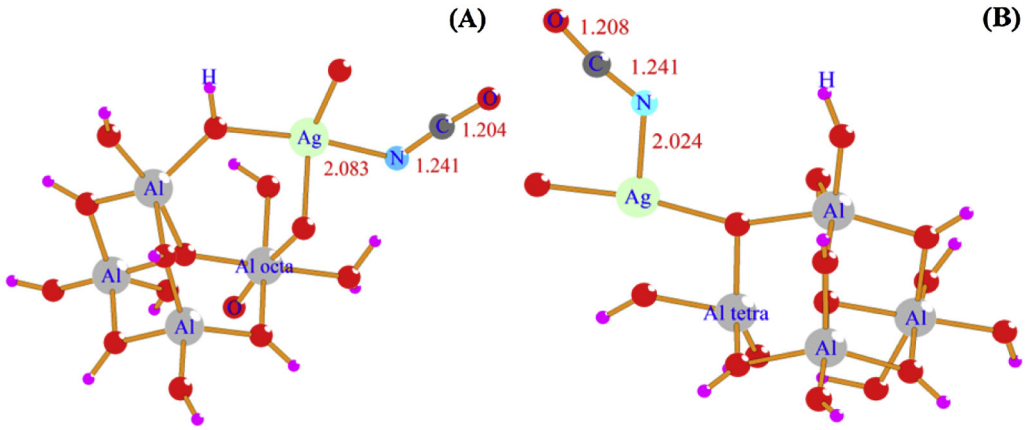

Fig. 3. Calculated models for the reaction of —NCO species on Ag/Al_2O_3 catalyst, (A) on Ag—O—Al_{octa} entity, (B) on Ag—O—Al_{tetra} entity.

Table 1
Calculated energies and vibrational stretching frequencies of —NCO and CNO— species on Ag/Al_2O_3 catalyst.

	Electronic and zero point energy (eV)	ν_{cal} (cm^{-1})	ν_{exp} (cm^{-1})	Ref	R(N=C) (Å)	R(C=O) (Å)	R(O=N) (Å)
OCN—Ag—O—Al_{octa}	−39,652.4	2248	2220	[17–22]	1.241	1.204	–
OCN—Ag—O—Al_{tetra}	−39,652.9	2221	−2260		1.241	1.208	–
CNO—Ag—O—Al_{octa}	−39,649.4	2102	2130	[23–25]	1.212	–	1.323
CNO—Ag—O—Al_{tetra}	−39,649.8	2105	−2160		1.211	–	1.328

between O=N and N=C are 1.200 and 1.116 Å, respectively. The structure parameters of the calculated models as shown in Table 1 agree closely with the results mentioned above.

Compared to isomers of adsorbed —NCO species, CNO— species are all weakly bound with silver ion species due to the relatively higher total energies as shown in Table 1. This suggests the CNO— species is unstable, and likely isomerizes to —NCO species through minimum energy principles. The IR frequency of CNO— species is at about 2100 cm^{-1}, which is close to the stretching vibration of —CN species according to extensive studies [19,22–25], and also confirmed by DFT calculation in supporting information (the vibrational frequency). Thus we can postulate that CNO— species may correspond to one kind of —CN species attached to a surface O atom. In a mixture of NO and O_2, —NCO and CNO— species possibly have different activity in the reduction of NO_x. Since CNO— species are barely observed in the HC-SCR process, we can conjecture that CNO— may highly active.

3.3. The activity of —NCO vs. CNO— toward NO_x

In order to compare the activity of Ag—O—Al_{octa} and Ag—O—Al_{tetra} entities, NCO— species adsorbed on these two active sites were calculated during NO_x reduction. NO_2 was selected as probe molecule rather than NO because it is more reactive [19]. Transition states of reaction between NO_2 and —NCO on different Ag—O—Al entities were searched. The energetic routes for reduction of NO_x by important intermediates are exhibited in Fig. 5.

We carefully compared the TSs for —NCO species on the two Ag—O—Al entities in reaction with NO_2 in Fig. 5(A). It is clear that the corresponding TSs on the two entities are very similar. NO_2 molecules collide with —NCO species adsorbed on the surface and finally yield N_2 and CO_2. The whole reaction on Ag—O—Al_{octa} and Ag—O—Al_{tetra} entities are exothermic, with reaction energies of −4.216 and −6.474 eV, respectively. The formation of N_2 and CO_2 on the Ag—O—Al_{tetra} entity is greatly enhanced over the Ag—O—Al_{octa} entity. The activation energy barriers for NO_2 + —NCO on Ag—O—Al_{octa} and Ag—O—Al_{tetra} entities are 0.462 and 0.299 eV, respectively. Thus we can conclude that the Ag—O—Al_{tetra} entity is thermodynamically and kinetically favorable, and should be the active site compared to the Ag—O—Al_{octa} entity.

To reveal the activity of isomers of —NCO and CNO— species toward NO_x, we investigated the energy route for the two surface intermediates toward NO_2 on the same active Ag—O—Al_{tetra} entity. Fig. 5(B) shows the energy route for NO_2 reacting with —NCO/CNO— species. Both reactions were exothermic, with the reaction energies of −6.474 for —NCO and −5.413 eV for CNO—, respectively,

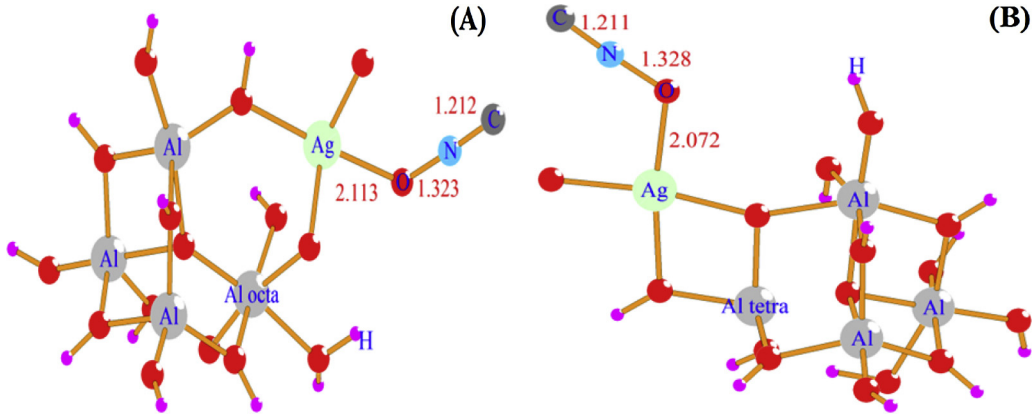

Fig. 4. Calculated models for the reaction of CNO— species on Ag/Al_2O_3 catalyst, (A) on Ag—O—Al_{octa} entity, (B) on Ag—O—Al_{tetra} entity.

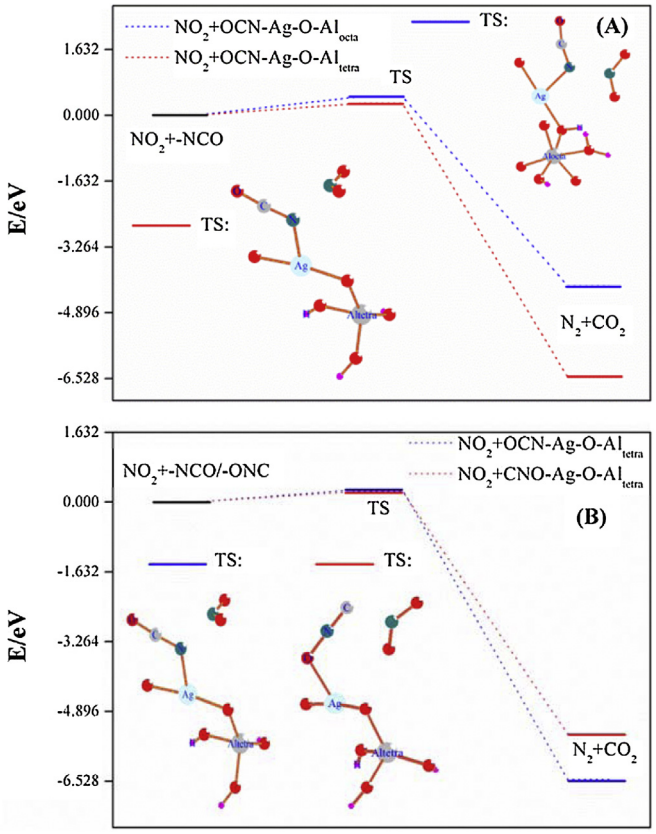

Fig. 5. Calculated barriers and reaction energies for NO_2 reacting with —NCO/CNO— species, (A) —NCO species on Ag—O—Al_{octa} and Ag—O—Al_{tetra} entity, (B) —NCO and CNO— species on Ag—O—Al_{tetra} entity.

indicating that the NO_2 reaction with —NCO species is energetically favored over CNO— species. We also searched the transition states for both reactions, which is also exhibited in Fig. 5(B). The activation energy barriers for NO_2 reacting with —NCO and CNO— on the Ag—O—Al_{tetra} entity are 0.299 and 0.245 eV, respectively. Therefore, CNO— species is slightly kinetically favorable over —NCO species to produce N_2 and CO_2 in reaction with NO_2. We demonstrated for the first time that the CNO— species might be one type of vital intermediate during the HC-SCR process. Static experimental methods have a difficult time capturing these features during the reduction of NO_x. However, based on DFT calculations, we unambiguously defined the species and compared the chemical features. In future study, we will explore the complete energy routes for activation of reductants and formation paths of vital intermediates.

4. Conclusions

Constructing an Ag/Al_2O_3 model with the density functional theory (DFT) method, good agreement was found between theoretical models and experimental characterization such as NMR and EXAFS. Ag—O—Al_{octa} and Ag—O—Al_{tetra} entities are the common types of silver ion species anchored on the Al_2O_3 surface and the Ag—O—Al_{octa} entity is energetically favorable. However, vital intermediates like —NCO species prefer to be adsorbed on the Ag—O—Al_{tetra} entity. Through searching the transition states of reaction between NO_2 and —NCO species adsorbed on two entities, we conclude that Ag—O—Al_{tetra} is more active and should be the true active site during HC-SCR. The CNO— species, as an isomer of —NCO, was found to be even more active for NO_x reduction over the site of the Ag—O—Al_{tetra} entity than —NCO species.

Acknowledgments

The work was supported by the National Natural Science Foundation of China (21373261 and 51221892), and the National High Technology Research and Development Program of China (863 Program, 2013AA065301).

Appendix A. Supplementary data

Supplementary data associated with this article can be found, in the online version, at http://dx.doi.org/10.1016/j.cattod.2015.03.023.

References

[1] R. Burch, J.P. Breen, F.C. Meunier, Appl. Catal. B 39 (2002) 283–303.
[2] K.-I. Shimizu, A. Satsuma, Phys. Chem. Chem. Phys. 8 (2006) 2677–2695.
[3] Z. Liu, S. Ihl Woo, Catal. Rev. 48 (2006) 43–89.
[4] H. He, X. Zhang, Q. Wu, C. Zhang, Y. Yu, Catal. Surv. Asia 12 (2008) 38–55.
[5] P. Granger, V.I. Parvulescu, Chem. Rev. 111 (2011) 3155–3207.
[6] F.C. Meunier, J.R.H. Ross, Appl. Catal. B 24 (2000) 23–32.
[7] K.A. Bethke, H.H. Kung, J. Catal. 172 (1997) 93–102.
[8] H. He, R.D. Zhang, Y.B. Yu, Chin. J. Catal. 24 (2003) 788–794.
[9] J.H. Li, R. Ke, W. Li, J.M. Hao, Catal. Today 139 (2008) 49–58.
[10] Z.M. Liu, J.H. Li, A.S.M. Junaid, Catal. Today 153 (2010) 95–102.
[11] Y.B. Yu, H. He, Q.C. Feng, J. Phys. Chem. B 107 (2003) 13090–13092.
[12] M. Haneda, Y. Kintaichi, Catal. Today 42 (1998) 127–135.
[13] S. Satokawa, J. Shibata, K. Shimizu, A. Satsuma, Appl. Catal. B 42 (2003) 179–186.
[14] X. She, M. Flytzani-Stephanopoulos, J. Catal. 237 (2006) 79–93.
[15] Y. Yan, Y.B. Yu, H. He, J. Catal. 293 (2012) 13–26.
[16] H. Deng, Y.B. Yu, F.D. Liu, J.Z. Ma, Y. Zhang, H. He, ACS Catal. 4 (2014) 2276–2784.
[17] J.W. London, A.T. Bell, J. Catal. 31 (1973) 96–109.
[18] Y. Ukisu, S. Sato, G. Muramatsu, K. Yoshida, Catal. Lett. 11 (1991) 177–182.
[19] S. Sumiya, H. He, A. Abe, N. Takezawa, K. Yoshida, Chem. Soc. J. Faraday Trans. 94 (1998) 2217–2219.
[20] T. Chafik, S. Kameoka, Y. Ukisu, T. Miyadera, J. Mol. Catal. A: Chem. 136 (1998) 203–211.
[21] S. Chansai, R. Burch, C. Hardacre, J. Breen, F. Meunier, J. Catal. 276 (2010) 49–55.
[22] S. Chansai, R. Burch, C. Hardacre, J. Breen, F. Meunier, J. Catal. 281 (2011) 98–105.
[23] S. Tamm, H.H. Ingelsten, A.E.C. Palmqvist, J. Catal. 255 (2008) 304–312.
[24] N. Bion, J. Saussey, M. Haneda, M. Daturi, J. Catal. 217 (2003) 47–58.
[25] F.T. Starzyk, E. Seguin, S. Thomas, M. Daturi, H. Arnolds, D.A. King, Science 324 (2009) 1048–1051.
[26] H. He, Y.B. Yu, Catal. Today 100 (2005) 37–47.
[27] A.L. Ankudinov, B. Ravel, J.J. Rehr, S.D. Conradson, Phys. Rev. B 58 (1998) 7565–7576.
[28] J.H. Kwak, J.Z. Hu, D.H. Kim, J.S. Szanyi, C.H.F. Peden, J. Catal. 251 (2007) 189–194.
[29] J.H. Kwak, J.Z. Hu, A. Lukaski, D.H. Kim, J.S. Szanyi, C.H.F. Peden, J. Phys. Chem. C 112 (2008) 9486–9492.
[30] J.H. Kwak, D.H. Mei, J. Catal. 261 (2009) 17–22.
[31] J.H. Kwak, J.Z. Hu, D.H. Mei, Science 325 (2009) 1670–1673.
[32] M. Digne, P. Sautet, P. Raybaud, P. Euzen, H. Toulhoat, J. Catal. 211 (2002) 1–5.
[33] M. Digne, P. Sautet, P. Raybaud, P. Euzen, H. Toulhoat, J. Catal. 226 (2004) 54–68.
[34] H. He, Y. Li, X.L. Zhang, Y.B. Yu, C.B. Zhang, Appl. Catal. A 375 (2010) 258–264.
[35] M.K. Kim, P.S. Kim, J.H. Baik, I.S. Nam, B.K. Cho, S.H. Oh, Appl. Catal. B 105 (2011) 1–14.
[36] J.P. Breen, R. Burch, C. Hardacre, C.J. Hill, J. Phys. Chem. B 109 (2005) 4805–4807.
[37] K.I. Shimizu, M. Tsuzuki, K. Kato, S. Yokota, K. Okumura, A. Satsuma, J. Phys. Chem. C 111 (2007) 950–959.
[38] S.T. Korhonen, A.M. Beale, M.A. Newton, B.M. Weckhuysen, J. Phys. Chem. C 115 (2011) 885–896.
[39] D. Britton, J.D. Dunitz, Acta Cryst. 18 (1965) 424.
[40] H.W. Gao, H. He, Spectrochim. Acta A 61 (2005) 1233–1238.
[41] A. Kecskemeti, T. Bagsagi, F. Solymosi, Catal. Lett. 116 (2007) 101–104.
[42] S. Zhao, Y.L. Ren, J.J. Wang, W.P. Yin, J. Mol. Struct.: Theochem. 897 (2009) 100–105.
[43] D. Britton, J.D. Dunitz, Acta Cryst. 19 (1965) 662–668.